https://doi.org/10.3311/PPch.45361
Creative Commons Attribution

Periodica Polytechnica Chemical Engineering

Utilizing UV-Sensitive Camera for UV-Reflectance-Imaging-Based Active Pharmaceutical Ingredient Content Prediction

Frida Barbara Molnar[1], Bence Szabó-Szőcs[1], Lajos Madarász[1*], Zsombor Kristóf Nagy[1], Dorián László Galata[2**], Attila Farkas[1], Lilla Alexandra Mészáros[1], György Marosi[1]

[1] Department of Organic Chemistry and Technology, Faculty of Chemical Technology and Biotechnology, Budapest University of Technology and Economics, Műegyetem rkp. 3., H-1111 Budapest, Hungary
[2] School of Engineering, University of Leicester, University Rd, LE1 7RH Leicester, United Kingdom
[*] Corresponding author, e-mail: madarasz.lajos@vbk.bme.hu
[**]Corresponding author, e-mail: dlg22@leicester.ac.uk

Received: 29 June 2026, Accepted: 28 September 2026, Published online: 16 November 2026

Abstract

This study presents a proof-of-concept monochrome camera system featuring a UV-sensitive sensor, enabling direct UV detection for non-destructive quantification of active pharmaceutical ingredient content in two-component canrenone-microcrystalline cellulose tablets. Differences in UV absorption between API and excipient resulted in distinct grayscale intensity distributions on the tablet surface, enabling active pharmaceutical ingredient (API) quantification. Tablets were prepared with API contents ranging from 0 to 6 w/w% and imaged in-line on a conveyor belt under 365 nm UV illumination. Acquired images were pre-processed through background elimination, and illumination correction, then grayscale intensity histograms were extracted. These histograms served as inputs for partial least squares regression, producing a linear correlation between predicted and nominal API content, with a root mean square error of calibration 0.20 w/w%, root mean square error of cross-validation 0.24 w/w%, root mean square error of prediction 0.27 w/w%. The obtained relative prediction error was 6.78% at a target of 4 w/w%. The approach demonstrates rapid, non-destructive assessment of API content without sample preparation. By combining a cost-effective direct UV-imaging method with multivariate analysis, the system shows potential for real-time monitoring of API content in continuous tablet manufacturing.

Keywords

UV reflectance imaging, API content prediction, machine vision, partial least squares, solid dosage forms, process analytical technology

1 Introduction

Quality-by-testing (QbT) is currently a widely used quality control strategy in pharmaceutical manufacturing, relying on a limited subset of samples subjected to slow, destructive offline testing [1]. Failure to meet specifications for critical parameters, such as active pharmaceutical ingredient (API) content, which directly impacts therapeutic performance and patient safety, can lead to the rejection of whole batches, potentially causing substantial financial loss [2].

To address these challenges, the concept of process analytical technology (PAT) was introduced to improve the understanding of pharmaceutical production processes and to enhance the efficiency of quality assurance. Over time, regulatory agencies have increasingly emphasized such modern approaches [3]), thus facilitating a shift toward PAT-based frameworks for the realization of Quality-by-Design (QbD), real-time release testing (RTRT) and continuous manufacturing [4].

Within the QbD framework, a comprehensive understanding of the effects of critical process parameters (CPPs) on critical quality attributes (CQAs) is crucial. CQAs describe the measurable properties that determine safety and efficiency of the product, while CPPs are the process variables that need to be carefully controlled to keep these attributes within the desired limits [5]. This is particularly relevant for solid oral dosage forms, which represent the majority of marketed pharmaceutical products [1, 6].

Among the CQAs of tablets API content and content uniformity are particularly significant, as they directly affect therapeutic performance, patient safety and the economic sustainability of production [7]. Despite the significant progress toward modernization, industrial quality

Cite this article as: Molnar, F. B., Szabó-Szőcs, B., Madarász, L., Nagy, Z. K., Galata, D. L., Farkas, A., Mészáros, L. A., Marosi, G. "Utilizing UV-Sensitive Camera for UV-Reflectance-Imaging-Based Active Pharmaceutical Ingredient Content Prediction", Periodica Polytechnica Chemical Engineering, 2026. https://doi.org/10.3311/PPch.45361

assurance still relies heavily on destructive, offline assays, that are time- and resource-intensive, limit sampling frequency and hinder the implementation of continuous, real-time feedback-controlled production processes [8].

Consequently, a broad range of non-destructive and real time techniques have emerged for tablet characterization within the PAT framework. Among these techniques near-infrared (NIR) spectroscopy is an established PAT tool that enables rapid, non-destructive spectral measurements suitable for in-line implementation in pharmaceutical manufacturing. NIR based models can be applied to predict CQAs from the acquired spectra, providing real-time process information. NIR spectroscopy has been extensively employed to quantify the API content and evaluate tablet hardness [9, 10], and it is officially accepted by the FDA as a PAT tool [11]. Furthermore, NIR and Raman spectroscopy combined with artificial neural network modelling have been used for the non-destructive prediction of tablet dissolution profiles, demonstrating their potential for real-time release testing [12].

In addition, transmission Raman spectroscopy (TRS) has also been applied to assess content uniformity, either in combination with NIRS [13] or as an independent technique [14]. TRS provides a large sampling volume, and sufficient optical penetration through both coating and core, enabling assessment of whole tablet API content and content uniformity. In the studies by Wang et al. [13] and Belay et al. [14], TRS was applied in an offline setting on tablet samples, demonstrating its capability for rapid, non-destructive bulk analysis of solid oral dosage forms.

Raman chemical imaging and mapping have also been investigated for the spatially resolved characterization of API distribution in pharmaceutical tablets. Farkas et al. applied Raman mapping and macropixel-based analysis to quantify the homogeneity of API distribution in tablets produced using both conventional and continuous processing technologies. Their results demonstrate that Raman imaging can provide quantitative information not only on the average API content, but also on its spatial distribution and homogeneity [15].

Beyond spectroscopic approaches, innovative non-destructive analytical tools have also been introduced, which utilize thermo-physical and afterglow-based responses. A thermal-conductivity-based approach was proposed, where amoxicillin concentration is predicted from heat transport characteristics [16]. Ultrabroadband carbon-nanotube-based photo-thermoelectric imagers operating from sub-terahertz to infrared wavelengths were reported for monitoring API content, and coating uniformity in-line [17]. Furthermore, an afterglow-driven tablet quality assessment was demonstrated using maltodextrin-based room-temperature phosphorescence, which complements and extends the range of available non-destructive methods for tablet quality assessment [18]. Other analytical techniques, such as inductively coupled plasma optical emission spectroscopy (ICP-OES), have also been applied in pharmaceutical analysis, for example, for elemental impurity profiling and multi-element characterization [19].

Similar to the mentioned innovative approaches, machine vision has become an increasingly important tool owing to its low investment cost, rapid data acquisition and great potential for integration into continuous manufacturing [20]. Visible-light illumination-based systems have been applied to monitor coloured APIs and excipients during granulation, blending and tableting [21]. However, their reliance on colour contrast makes them unsuitable for predicting the concentration of colourless APIs.

To overcome this limitation ultraviolet (UV) fluorescent-based imaging has been introduced as a non-destructive and fast inspection method. By illuminating dosage forms with a specific wavelength range, differences in fluorescence and absorption can generate sufficient contrast for API content prediction using RGB cameras [22, 23]. Recent studies have proved that UV imaging can sufficiently predict API content and related tablet properties, thus the applicability of image-based methods can be extended to colourless APIs [23, 24].

However, some APIs may not exhibit fluorescence, which could limit the broader applicability of this fluorescence-based methodology. To address this, we propose the application of a camera equipped with a monochrome CMOS sensor sensitive in the 200–1100 nm wavelength range [25], enabling the absorbance-based detection of many clinically relevant APIs on the WHO Model List of Essential Medicines [26] that predominantly act as strong UV absorbers due to their aromatic or conjugated structures [27]. The mentioned sensor could detect direct UV light and has already been utilised elsewhere [28]. This sensor represents a potential new prospect for pharmaceutical applications.

This study aims to demonstrate the potential applicability of UV-reflectance imaging using a novel camera system for the non-destructive prediction of API content in tablets. The setup uses an UV camera with a specific sensor (range 200–1100 nm) combined with a quartz objective and 365 nm UV illumination, to explore the applications of the mentioned sensor in a pharmaceutical quality

assessment task. In this proof-of-concept study, we aim to showcase the feasibility and potential of UV-reflectance detection in the pharmaceutical manufacturing by using it to evaluate the API content of tablet cores.

2 Materials and methods

2.1 Materials

Canrenone, primarily used as an anti-mineralocorticoid drug and diuretic, was chosen as a model API and was obtained from Sigma-Aldrich (St. Louis, Missouri, USA). Microcrystalline cellulose (MCC, Vivapur® 200) used as an excipient, was purchased from JRS Pharma (Rosenberg, Germany).

2.2 Methods

2.2.1 Preparation of the sample set

Tablets with a target weight of 100 ± 10 mg were produced using a Dott Bonapace CPR-6 (Limbiate, Italy) single punch tablet press equipped with 8 mm diameter flat punches. The compression force was set to 11 kN. Seven groups of tablets were prepared; each contained a varying canrenone dosage between 0–6 w/w% (weight/weight percent). The MCC content was altered accordingly. 5 g mixtures were prepared for each content level and were manually homogenized for 10 min prior to tabletting. In total, 32 samples were prepared with varied API content levels. The samples are summarized in Table 1 for the calibration and validation sample sets. The target API content was set by the authors at 4 w/w%.

In addition to the samples used for partial least squares (PLS) model development and validation, supplementary sample set with canrenone contents above 6 w/w% and up to 10 w/w% were prepared in preliminary experiments under the same tableting conditions to investigate the response behaviour of the UV-reflectance imaging approach at higher API content levels. These samples are shown in Table 2.

Table 1 The theoretical API content of samples in calibration and test sets

Theoretical API content (w/w%)	Number of samples in the calibration set	Number of samples in the test set
0	5	0
1	4	0
2	3	1
3	4	1
4	3	2
5	3	1
6	5	0

Table 2 Supplementary sample set for the evaluation of UV-reflectance imaging response at higher API contents

Theoretical API content (w/w%)	Number of samples in the test
6	5
7	4
8	5
9	5
10	4

2.2.2 UV-reflectance imaging setup

An Allied Vision Alvium 1800 U-812 UV camera (Stadtroda, Germany) was used for image acquisition, equipped with a fixed, 25 mm focal length quartz objective (Edmund optics, Barrington, USA). Between the camera and the objective, a 5 mm spacer (Edmund optics, Barrington, USA) was inserted. The camera incorporates the Sony IMX487 CMOS sensor, a recent monochrome global shutter imager with a spectral range extending from 200–1100 nm, enabling enhanced UV performance. Compared to conventional VIS sensors, this provides superior quantum efficiency in the UV range. This monochrome configuration yields higher contrast and spatial resolution in UV-imaging, rendering it suitable for non-destructive tablet analysis [25].

The camera was connected to the computer via a USB 3.0 port. UV illumination was provided by a ring light (VastFire, China) emitting light at ~365 nm. The imaging process was conducted in a dark room to exclude ambient light interference. The exposure time was set to 690 µs. Images were taken from both sides of the tablets at a resolution of 2114 × 1800 pixels.

To simulate the execution of a modern quality assessment task real-time UV-reflectance imaging was performed using the setup shown in Fig. 1, which provides

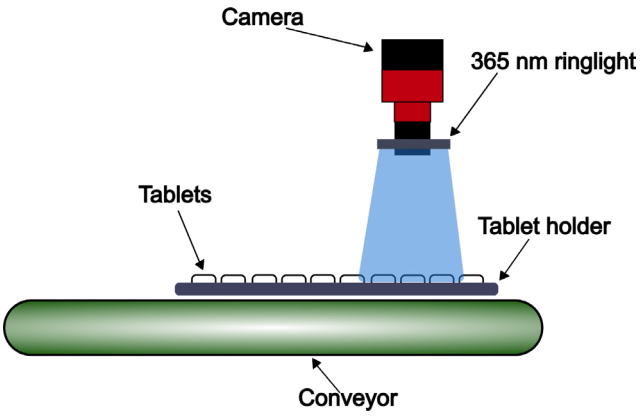


Fig. 1 The configuration of the image acquisition

a side view of the configuration of the system. For better positioning, 10 tablets were placed in a holder specifically designed and 3D-printed, arranged in a single row with 5 mm spacing between each tablet. Then the holder was moved using conveyor belt at a speed of 0.206 m/s. Image acquisition was carried out at a frame rate of 30 frames/s. Subsequently, the acquired samples were carefully collected in a predefined sequence to align with the theoretical API content.

2.2.3 Development of the algorithm for image processing

To predict the API content of the prepared tablets, an algorithm was developed in MATLAB R2024b (Matlab2024b, MathWorks, Natick, MA, USA) [29] runtime environment. The scheme of the algorithm is shown in Fig. 2.

The image processing pipeline standardizes the acquired images by integrating the determination of the region of interest and illumination correction. After importing the image set, tablets were detected using a Hough transform-based circle detection. Following this, the detected parameters were employed to generate a mask for eliminating the regions out of the sample. The detected circle was then cropped, resized to a fixed resolution with the width and height of 512 pixel, and refined by morphological operations. Subsequently, a distance-transform-based circular crop produced a centrally aligned, ideal circular mask, ensuring geometric consistency across samples.

Illumination correction was executed by estimating smooth background illumination via Gaussian filtering. The original images were divided by these background estimates to compensate for non-uniform illumination. The resultant images were normalized by the mean intensity within the mask and placed onto a white background to eliminate residual artifacts. Pixel intensities inside the mask were extracted from the final corrected images normalized to a 0–1 range using linear scaling and summarized in histograms, which can be rescaled to the 0–255 range if needed. These histograms served as illumination- and position-invariant descriptors for further analysis.

2.2.4 Application of multivariate data analysis in the prediction of active pharmaceutical ingredient content

For the prediction of API content PLS regression was conducted with PLS Toolbox 9.2 (Eigenvector Research, Manson, WA, USA) [30].

After image processing, the obtained histograms were smoothed (smoothing filter, order 2 window 25 pt tails: polyinterp), followed by mean centering. The theoretical API content of the tablets was used as the response variable. In the calibration procedure, a contiguous block cross-validation method with 10 splits was used. The genetic algorithm (GA) selected variables to enhance the predictive ability of the models. GAs were run with a population size of 150, a variable window width of 16 and a maximum latent variable (LV) number of 6. The best model was chosen from three replicate runs. To prevent overfitting the best model was chosen based on the lowest number of LVs. The models were evaluated using goodness parameters of root mean square error of calibration (RMSEC), root mean

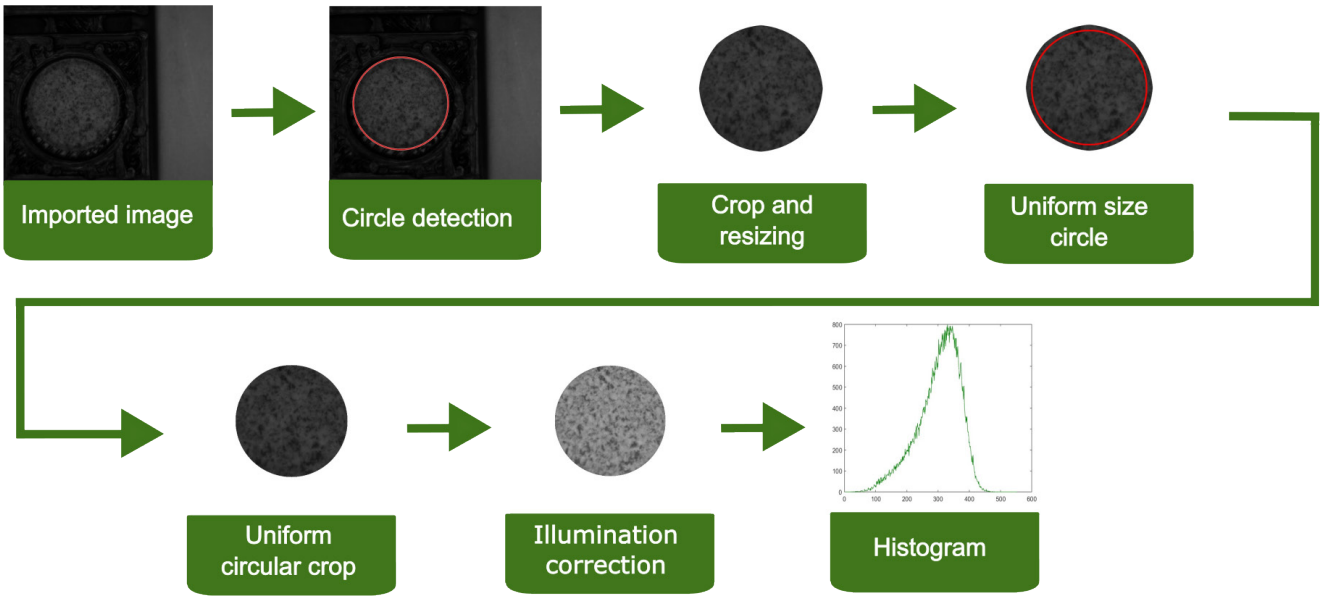


Fig. 2 The steps of the developed image processing algorithm

square error of cross-validation (RMSECV), root mean square error of prediction (RMSEP), coefficient of determination for calibration (R^2C) and coefficient of determination for cross-validation (R^2CV).

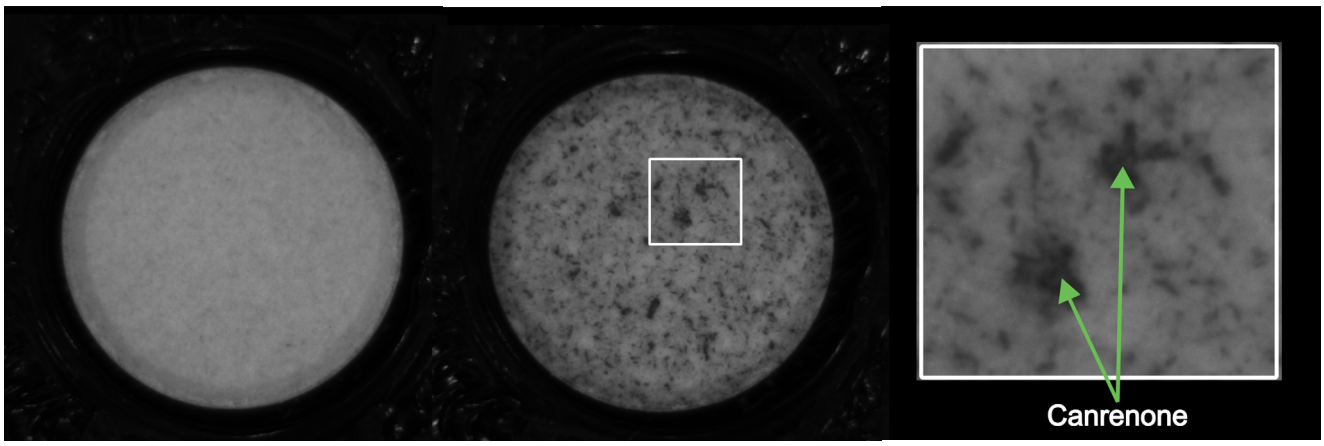
3 Results and discussion

3.1 Assessment of the appearance of the components and the prepared tablets

To initially assess the surface appearance of the individual components with UV-reflectance imaging, a neat MCC tablet and a 4 w/w% MCC-canrenone-containing tablet were analysed as shown in Fig. 3. Visual inspection of the acquired images revealed that the two components exhibit distinct regions, as their grayscale intensity distributions differ from each other. This distinction arises because canrenone more strongly absorbs 365 nm UV photons due to its conjugated structure, appearing darker in the images and thereby enabling its differentiation from MCC.

To perform a preliminary evaluation of the applicability of direct UV imaging in the prediction of canrenone content in the prepared tablets, three samples with varying amounts of API content were analysed, as shown in Fig. 4.

On these UV-reflectance images, it can be observed that tablets containing higher dosage of canrenone have a darker hue, with the 6 w/w% tablet appearing the darkest and the 2 w/w% the brightest, reflecting the visible presence of the API (Fig. 4). Accordingly, the API content of the tablets could be predictable, as indicated by the darkening of the tablets, resulting with the application of ~365 nm UV illumination. A potential correlation between API content and corresponding changes in light response may enable the non-destructive quantification of the mentioned parameter.



(a) (b) (c)

Fig. 3 The appearance of an MCC (a), an MCC-canrenone (b) containing sample and an enlarged region (c) denoted with white rectangle on the sample surface

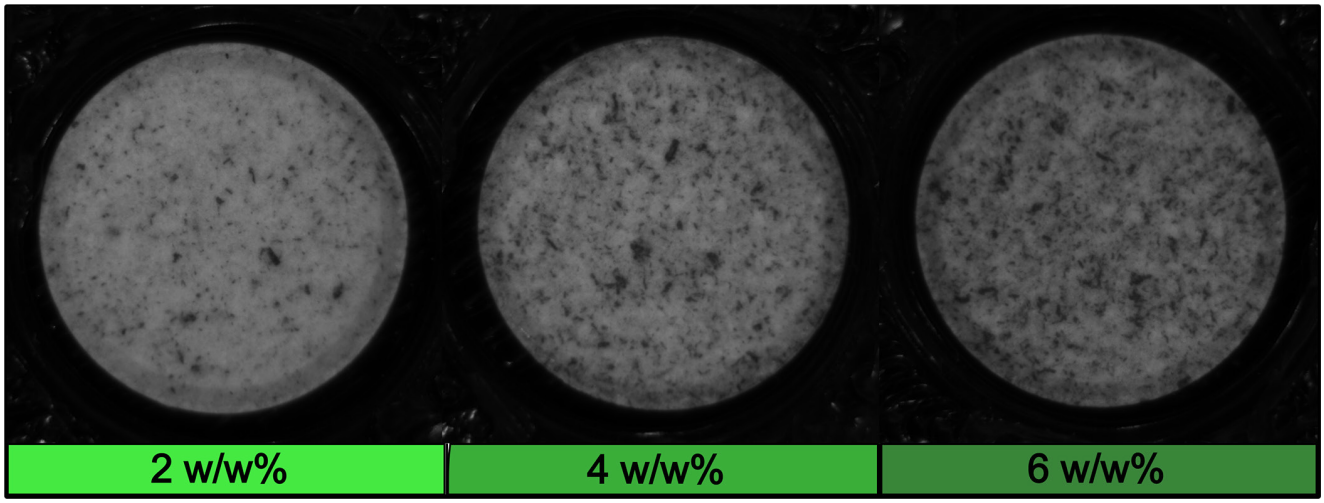


Fig. 4 The appearance of the surface of the samples with varying canrenone content

3.2 Generation of the input dataset

To establish the input dataset for the calibration procedure, histograms were created from the images acquired on both sides of each sample (see Section 2.2.3). For each group, the corresponding histograms were averaged in order to reduce variability and obtain representative distributions. The resulting mean histograms are summarized in Fig. 5.

An evaluation of average histograms for canrenone tablets with varying API content (Fig. 5) reveals a systematic trend. With increasing API content, the histograms become progressively broader and flatter after the applied image processing steps. This behaviour is consistent with the visual appearance of the samples, higher canrenone content result in a darker and more heterogeneous tablet surface. This effect can be attributed to the increasing number of API particles on the surface which absorb a larger fraction of the incident UV light.

Due to the normalization step applied during illumination correction, the histograms are centred to a comparable intensity level. Consequently, the primary differences between the API content levels are reflected in the width and shape of the intensity distributions.

During preliminary method-development experiments to optimize the imaging conditions, samples with canrenone contents above 6 w/w% were also evaluated (Fig. 6). These preliminary measurements showed substantially reduced concentration-dependent differentiation at higher API contents. Based on these observations, the 0–6 w/w% range was selected for subsequent proof-of-concept quantitative modelling. The higher-content preliminary samples were used only to support selection of the modelling range and were not included in the final PLS calibration or validation datasets.

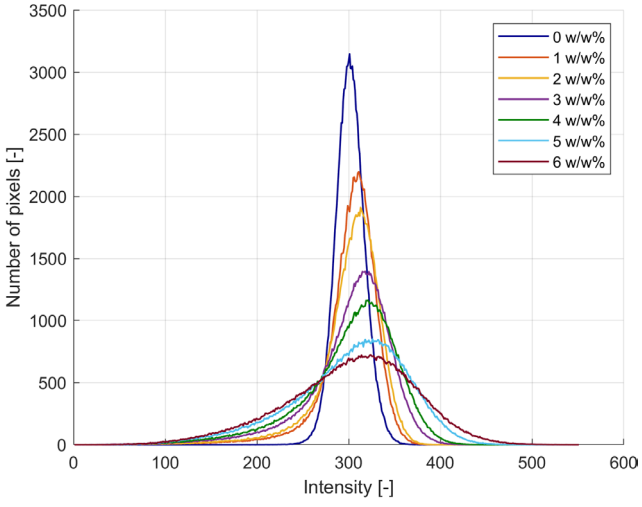


Fig. 5 The average histograms of the applied dosage groups of the sample set

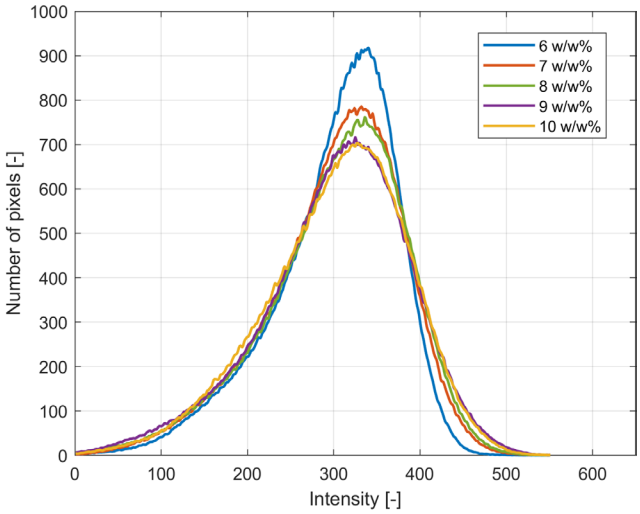


Fig. 6 Average histograms of samples containing 6–10 w/w% canrenone obtained during preliminary method-development experiments

Importantly, the reduced differentiation observed at higher canrenone contents reflects the response behaviour of the present API–excipient system and imaging configuration and should not be interpreted as a general upper concentration limit of UV-reflectance imaging.

The systematic variations between histograms at 0–6 w/w% range suggest that the extracted features may serve as suitable input variables for the development of a PLS model.

3.3 Development of the partial least squares model

The prepared 32 samples constituted the dataset for the API content prediction model. The elements of the sample sets were randomly split, with 27 tablets allocated to calibration and 5 to validation. The result of the calibration is shown in Fig. 7.

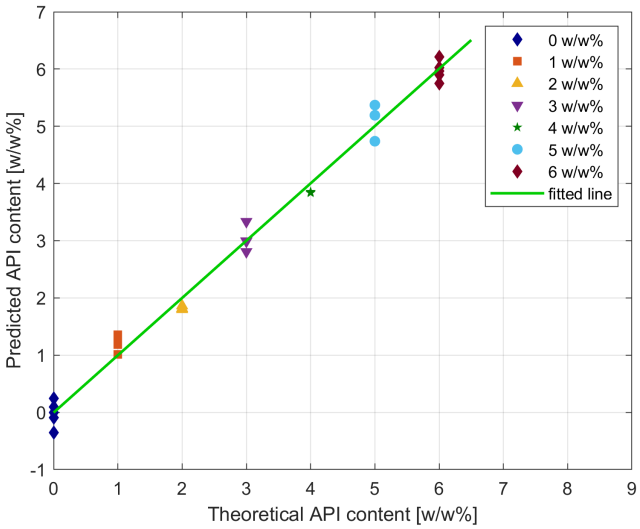


Fig. 7 The obtained PLS model for the prediction of API content

It can be observed that the correlation between the predicted and theoretical API content appears to be linear within the analysed range. The fitted line is close to the ideal 1:1 relationship with the equation of $y = 0.992x - 0.007$. The slope and intercept of the regression line were statistically evaluated using *t*-tests against the null hypotheses that the slope equals 1 and the intercept equals 0 ($\alpha = 0.05$). The obtained *p*-values were 0.67 for the slope and 0.92 for the intercept, indicating that no statistically significant deviations were detected. Some variability can be observed within the content groups, which may arise from natural tablet-to-tablet heterogeneity and minor variations in composition. However, these variations remain relatively small and do not substantially affect the overall linear correlation between the predicted and theoretical API contents.

The PLS model utilized 2 LVs, achieving an RMSEC of 0.20 w/w% and an RMSECV of 0.24 w/w%. These values show a small difference, which does not indicate overfitting and suggests potentially good generalisation to future samples. The reached R^2C of 0.99 and R^2CV of 0.99 further indicate that the built PLS model has reliable predictive performance for the API content determination in the validation set. Overall, the results suggest that the extracted histogram features contain relevant information on canrenone content and that the applied preprocessing steps were suitable for the model generation.

3.4 Test of the created model for the prediction of API content

The test samples aligned with the calibration curve, falling within the observed linear correlation. As the same calibration regression line is shown in Figs. 7 and 8, the statistical validation described above also applies to the regression line presented in Fig. 8. As previously mentioned, the slope did not differ significantly from one and the intercept did not differ significantly from zero, confirming that the calibration line did not differ significantly from the ideal 1:1 relationship. The test samples aligned with the calibration, fitting within the observed linear correlation. Different API content levels form visually distinct groups without overlap, indicating discrimination between the predicted API content levels. Fig. 8 includes both the samples used for model calibration and the test samples, providing a direct comparison between the model and test samples. The largest deviations from the theoretical values in the test set are observed for the 2 and 5 w/w% tablets, while the other concentration levels show smaller differences between predicted and theoretical API contents.

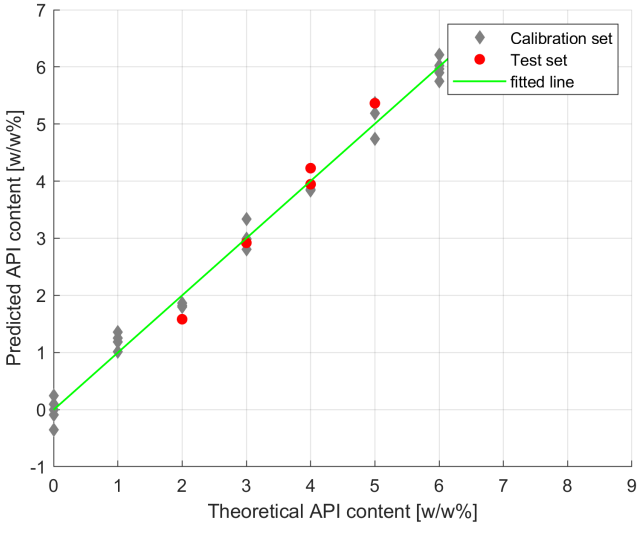


Fig. 8 The obtained result for the test sample set

Table 3 showcases the theoretical and predicted API content of the test sample set. In order to assess the performance of the method, the RMSEP was calculated. The obtained RMSEP was 0.27 w/w%, yielding an error of 6.78% of relative to the target dosage of 4 w/w%. The RMSEP is close to the RMSEC, which indicates no overfitting in the model, and the low relative error suggests that the model performs well on previously unexamined tablets. Considering these results, at a proof-of concept level, the presented UV-reflectance-based machine vision approach shows promising capability for predicting the API content.

In the following the UV-reflectance-imaging-based model is placed in context by comparing its goodness parameters with published PAT applications used for quantitative analysis. The aim is to evaluate whether the achieved accuracy and error levels fall within the performance range reported for other PAT tools within solid dosage forms and powder forms.

Published studies generally report high coefficients of determination in the range of 0.95–0.99 and relative prediction errors in the low- to mid-single-digit percentage range of 3–7%, which are similar to performance metrics obtained for the present model. Within this broader

Table 3 The theoretical and the predicted API content and their difference for the samples of the test set

Theoretical API content [w/w%]	Predicted API content [w/w%]	Difference [w/w%]
2	1.582	0.418
3	2.920	−0.080
4	3.945	−0.055
4	4.227	0.227
5	5.364	0.364

context, the predictive performance observed for the present model can be considered comparable to that typically achieved by established PAT approaches [23, 24, 31–33].

Overall, the results suggest that the obtained imaging-based model operates within the expected goodness parameters of quantitative PAT methods. The observed prediction error does not indicate a substantial deviation from commonly accepted performance levels, supporting the potential applicability quantitative pharmaceutical analysis.

3.5 Discussion of applicability

The quantitative response range of UV-reflectance imaging is expected to depend on the investigated API-excipient system and the applied imaging and data-processing conditions. In the presented canrenone–MCC system, systematic concentration-dependent changes in the image-derived histograms were observed within the 0–6 w/w% range, whereas the supplementary samples containing 6–10 w/w% canrenone showed progressively reduced differentiation between concentration levels. Notably, the correlation between grayscale intensities and API content may only be linear within a specific API content range. More API particles on the surface absorb greater amounts of UV light, making the tablet appear darker. However, this darkening phenomenon can become undetectable when exceeding a certain API content. Consequently, the correlation is no longer linear and instead follows a saturation-like tendency potentially compromising predictive accuracy at higher API levels [34].

The applicable quantitative range may vary depending on factors such as the UV absorption properties of the API and excipients, formulation composition, illumination wavelength, imaging conditions, and the applied data-processing strategy.

Tablets exhibiting a more inhomogeneous particle distribution and larger agglomerates on their surface tend to yield higher API content predictions because more particles make the tablet surface darker due to the UV absorption of the API. Thus, the proposed method can also potentially be utilized for homogeneity assessment. Moreover, although exposure times are short, prolonged or repeated UV illumination could theoretically induce photodegradation of some APIs. This necessitates careful validation of UV-sensitive compounds and the precise selection of illumination time.

Another concern is the size and structure of the dataset used for the model development. Increasing the number of tablets at each level and using a fully balanced calibration and validation dataset would further improve the robustness of the model. The present study was designed as a proof-of-concept to demonstrate the feasibility of UV-reflectance imaging for API content prediction rather than to provide a full analytical validation of the PLS model. Therefore, the robustness and generalisability of the presented model should be confirmed using a larger and balanced dataset in future studies

The potential applicability of the method extends to a broad range of APIs, as most of them are UV-active. Before transferring the imaging-based method to an other API, preliminary experiments are essential to confirm sufficient contrast between the API and the excipients. Furthermore, grayscale images can provide less information compared to RGB images. Adjusting the illumination wavelength may enable the inspection of tablets, in which the API is not distinguishable from the excipients under 365 nm UV illumination. This flexibility enhances the versatility of the method for both qualitative and quantitative analysis. Further studies could investigate the potential effects of tablet curvature and surface roughness on the measured reflectance.

Additionally, direct reflection-based UV imaging allows very short exposure times, such as 690 µs used in the present study, in similar systems could be faster than fluorescence, which often requires several ms/frame [35]. In fluorescence, the signal arises from weaker emitted light with lower intensity. Reflected UV, however, captures the strong incident light directly, the API appears dark against bright, reflective excipients.

The presented approach can offer rapid, non-destructive analysis that eliminates the need for sample preparation. Beyond API content determination, it reveals the size distribution of the API within tablets, providing valuable additional insights such as potentially predicting dissolution profiles. This could support more comprehensive quality assessment in pharmaceutical manufacturing.

4 Conclusion

This study demonstrates the potential applicability of UV-reflectance imaging using a novel camera system based on the UV-sensitive sensor for non-destructive API content prediction in canrenone-containing tablets at a proof-of-concept level. The evaluation workflow closely follows general image analysis and PLS-based chemometric practice. The novelty of this method involves the use of the UV sensor and optical setup, including the quartz objective and ~365 nm illumination. Across the investigated content range of 0–6 w/w%, the calibration showed a linear correlation between predicted and theoretical API content, with RMSEC of 0.20 w/w%, RMSECV of 0.24 w/w%, RMSEP of 0.27 w/w% and a relative error of 6.78%.

The presented approach offers clear advantages. It provides rapid, non-destructive, sample preparation-free measurement of API content using relatively simple image acquisition and data analysis steps. The overall system cost is expected to be lower than that of NIR or Raman based PAT solutions, while achieving similar predictive performance. Future improvements could involve additional evaluation methods to enhance the performance or using determined content values. In conclusion the quality of the information retrieved from the acquired images and the obtained results indicate that the presented UV-reflectance-imaging-based method has strong potential to be a practical PAT tool for API content prediction.

Acknowledgement

The project was supported by the János Bolyai Research Scholarship of the Hungarian Academy of Sciences. The research has been implemented with the support provided by the Ministry of Innovation and Technology of Hungary from the National Research, Development and Innovation Fund, financed under the [K-143039] funding scheme. This project has received funding from the European Union's Horizon Europe research and innovation programme under the Marie Skłodowska-Curie grant agreement No 101207440. Supported by the DKÖP-25-1-BME-32 University Research Scholarship Program of the Ministry for Culture and Innovation from the source of the National Research, Development and Innovation Fund. Project no. EKÖP-25-4-II-BME-91 has been implemented with the support provided by the Ministry of Culture and Innovation of Hungary from the National Research, Development and Innovation Fund, financed under the EKÖP-25 funding scheme.

References

[1] Nagy, B., Galata, D. L., Farkas, A., Nagy, Z. K. "Application of Artificial Neural Networks in the Process Analytical Technology of Pharmaceutical Manufacturing—a Review", The AAPS Journal, 24(4), 74, 2022. https://doi.org/10.1208/s12248-022-00706-0

[2] Rossi, C. V. "A Comparative Investment Analysis of Batch Versus Continuous Pharmaceutical Manufacturing Technologies", Journal of Pharmaceutical Innovation, 17(4), pp. 1373–1391, 2022. https://doi.org/10.1007/s12247-021-09612-y

[3] U.S. Department of Health and Human Services, Food and Drug Administration, Center for Drug Evaluation and Research (CDER), Center for Veterinary Medicine (CVM), Office of Regulatory Affairs (ORA) "PAT — A Framework for Innovative Pharmaceutical Development, Manufacturing, and Quality Assurance", FDA, Rockville, MD, USA, FDA-2003-D-0032, 2004. [online] Available at: https://www.fda.gov/regulatory-information/search-fda-guidance-documents/pat-framework-innovative-pharmaceutical-development-manufacturing-and-quality-assurance [Accessed: 16 December 2025]

[4] Yang, S., Hu, X., Zhu, J., Zheng, B., Bi, W., Wang, X., Wu, J., Mi, Z., Wu, Y. "Aspects and Implementation of Pharmaceutical Quality by Design from Conceptual Frameworks to Industrial Applications", Pharmaceutics, 17(5), 623, 2025. https://doi.org/10.3390/pharmaceutics17050623

[5] Démuth, B., Fülöp, G., Kovács, M., Madarász, L., Ficzere, M., …, Nagy, Z. K. "Continuous Manufacturing of Homogeneous Ultralow-Dose Granules by Twin-Screw Wet Granulation", Periodica Polytechnica Chemical Engineering, 64(4), pp. 391–400, 2020. https://doi.org/10.3311/PPch.14972

[6] Arioz, E., Ogunc, M. "Development of Starch-based Orodispersible Films for Paracetamol Delivery: A Comparative Study", Periodica Polytechnica Chemical Engineering, 69(4), pp. 525–536, 2025. https://doi.org/10.3311/PPch.42034

[7] Forbes, T. P.,Agolini, O., Altamimi, Z., Lawrence, J. "Personalized medicine: a quality by design approach to printable tablet production", RSC Pharmaceutics, 2(5), pp. 1096–1109, 2025. https://doi.org/10.1039/d5pm00041f

[8] Celikovic, S., Rehrl, J., Fraga, R. M., Steinberger, M., Khinast, J., Horn, M., Sacher, S. "A modern strategy for digital real-time release testing in continuous tablet manufacturing", European Journal of Pharmaceutics and Biopharmaceutics, 211, 114700, 2025. https://doi.org/10.1016/j.ejpb.2025.114700

[9] Kandpal, L. M., Tewari, J., Gopinathan, N., Stolee, J., Strong, R., Boulas, P., Cho, B.-K. "Quality assessment of pharmaceutical tablet samples using Fourier transform near infrared spectroscopy and multivariate analysis", Infrared Physics & Technology, 85, pp. 300–306, 2017. https://doi.org/10.1016/j.infrared.2017.07.016

[10] De Man, A., Uyttersprot, J.-S., Chavez, P.-F., Vandenbroucke, F., Bovart, F., De Beer, T. "The application of Near-Infrared Spatially Resolved Spectroscopy in scope of achieving continuous real-time quality monitoring and control of tablets with challenging dimensions", International Journal of Pharmaceutics, 641, 123064, 2023. https://doi.org/10.1016/j.ijpharm.2023.123064

[11] U.S. Department of Health and Human Services, Food and Drug Administration, Center for Drug Evaluation and Research (CDER) "Development and Submission of Near Infrared Analytical Procedures Guidance for Industry", FDA, Rockville, MD, USA, FDA-2015-D-0868, 2021. [online] Available at: https://www.fda.gov/regulatory-information/search-fda-guidance-documents/development-and-submission-near-infrared-analytical-procedures [Accessed: 02 February 2026]

[12] Péterfi, O., Nagy, Z. K., Sipos, E., Galata, D. L. "Artificial Intelligence-based Prediction of *In Vitro* Dissolution Profile of Immediate Release Tablets with Near-infrared and Raman Spectroscopy", Periodica Polytechnica Chemical Engineering, 67(1), pp. 18–30, 2023. https://doi.org/10.3311/PPch.20755

[13] Wang, X., Mao, D.-Z., Yang, Y.-J. "Calibration transfer between modelled and commercial pharmaceutical tablet for API quantification using backscattering NIR, Raman and transmission Raman spectroscopy (TRS)", Journal of Pharmaceutical and Biomedical Analysis, 194, 113766, 2021. https://doi.org/10.1016/j.jpba.2020.113766

[14] Belay, N. F., Busche, S., Manici, V., Shaukat, M., Arndt, S.-O., Schmidt, C. "Evaluation of Transmission Raman spectroscopy and NIR Hyperspectral Imaging for the assessment of content uniformity in solid oral dosage forms☆", European Journal of Pharmaceutical Sciences, 166, 105963, 2021. https://doi.org/10.1016/j.ejps.2021.105963

[15] Farkas, A., Nagy, B., Marosi, G. "Quantitative Evaluation of Drug Distribution in Tablets of Various Structures via Raman Mapping", Periodica Polytechnica Chemical Engineering, 62(1), pp. 1–7, 2018. https://doi.org/10.3311/PPch.10143

[16] Surangsrirat, D., Srikun, O., Sangawitayakorn, C., Wannasetdecho, T., Puanglamjeak, M., Birdi, P., Kirkup, J., Chana, K. "Nondestructive Measurement Technique for Substandard Amoxicillin Based on Thermal Approach", ACS Omega, 9(17), pp. 19378–19384, 2024. https://doi.org/10.1021/acsomega.4c00536

[17] Kubota, M., Kinoshita, Y., Hirokawa, S., Shikichi, D., Izumi, N., …, Li, K. "In-line multi-wavelength non-destructive pharma quality monitoring with ultrabroadband carbon nanotubes photo-thermoelectric imaging scanners", Light: Science & Applications, 14(1), 306, 2025. https://doi.org/10.1038/s41377-025-01957-0

[18] Li, Z., Xiong, H., Zhu, W., Zhong, Z., Li, Q., …, Ming, L. "Afterglow-driven tablet quality assessment: non-destructive detection via maltodextrin-based room temperature phosphorescence", International Journal of Pharmaceutics, 684, 126114, 2025. https://doi.org/10.1016/j.ijpharm.2025.126114

[19] Kakuk, M., Farkas, D., Kállai-Szabó, B., Pencz, K., Mészáros, L. A., Tonka-Nagy, P. G., Kállai-Szabó, N., Antal, I. "Inductively Coupled Plasma Optical Emission Spectroscopy (ICP-OES): Exploring Versatile Applications in Industrial and Analytical Fields", Periodica Polytechnica Chemical Engineering, 69(2), pp. 339–360, 2025. https://doi.org/10.3311/PPch.40025

[20] Galata, D. L., Mészáros, L. A., Kállai-Szabó, N., Szabó, E., Pataki, H., Marosi, G., Nagy, Z. K. "Applications of machine vision in pharmaceutical technology: A review", European Journal of Pharmaceutical Sciences, 159, 105717, 2021. https://doi.org/10.1016/j.ejps.2021.105717

[21] Ficzere, M., Mészáros, L. A., Madarász, L., Novák, M., Nagy, Z. K., Galata, D. L. "Indirect monitoring of ultralow dose API content in continuous wet granulation and tableting by machine vision", International Journal of Pharmaceutics, 607, 121008, 2021. https://doi.org/10.1016/j.ijpharm.2021.121008

[22] Alexandra Mészáros, L., Madarász, L., Kádár, S., Ficzere, M., Farkas, A., Kristóf Nagy, Z. "Machine vision-based non-destructive dissolution prediction of meloxicam-containing tablets", International Journal of Pharmaceutics, 655, 124013, 2024. https://doi.org/10.1016/j.ijpharm.2024.124013

[23] Ficzere, M., Alexandra Mészáros, L., Diószegi, A., Bánrévi, Z., Farkas, A., Lenk, S., László Galata, D., Kristóf Nagy, Z. "UV imaging for the rapid at-line content determination of different colourless APIs in their tablets with artificial neural networks", International Journal of Pharmaceutics, 657, 124174, 2024. https://doi.org/10.1016/j.ijpharm.2024.124174

[24] Ficzere, M., Diószegi, A., Farkas, A., Weiss, B., Mészáros, L. A., Nagy, Z. K. "High throughput in-line content uniformity measurement of tablets based on real-time UV imaging", International Journal of Pharmaceutics, 669, 125066, 2025. https://doi.org/10.1016/j.ijpharm.2024.125066

[25] Allied Vision "Alvium 1800 U-812 UV", [pdf] 2025. Available at: https://www.alliedvision.com/assets/support/Camera-Documentation/Allied-Vision/Cameras/Alvium/Alvium-USB/Data-Sheets/Alvium_1800_U-812_UV_DataSheet_en.pdf [Accessed: 22 January 2026]

[26] World Health Organization "EML – Model List of Essential Medicines", [online] Available at: https://list.essentialmeds.org/ [Accessed: 16 December 2025]

[27] Escayola, S., Labella, J., Szczepanik, D. W., Poater, A., Torres, T., Solà, M., Matito, E. "From (Sub)Porphyrins to (Sub)Phthalocyanines: Aromaticity Signatures in the UV–Vis Absorption Spectra", Inorganic Chemistry, 63(39), pp. 18251–18262, 2024. https://doi.org/10.1021/acs.inorgchem.4c03139

[28] DeLeon, C. M., Kupinski, M. "Ground-based ultraviolet polarimetry for imaging the Babinet polarization neutral point", Optical Review, 32(2), pp. 372–380, 2025. https://doi.org/10.1007/s10043-025-00958-z

[29] The MathWorks, Inc. "MATLAB, (R2024b)", [computer program] Available at: https://www.mathworks.com/products/new_products/release2024b.html [Accessed: 16 December 2025]

[30] Eigenvector Research, Inc. "PLS_Toolbox, (9.2)", [computer program] Available at: https://eigenvector.com/software/pls-toolbox/ [Accessed: 16 December 2025]

[31] Péter-Haraszti, A., Bakucz, L. G., Mészáros, L. A., Záhonyi, P., Szabó, E. "Drug content determination of amorphous solid dispersion containing tablets using a non-destructive and rapid UV imaging method", International Journal of Pharmaceutics, 678, 125726, 2025. https://doi.org/10.1016/j.ijpharm.2025.125726

[32] Mészáros, L. A., Gyürkés, M., Varga, E., Tacsi, K., Honti, B., Borbás, E., Farkas, A., Nagy, Z. K., Nagy, B. "Real-time release testing of *in vitro* dissolution and blend uniformity in a continuous powder blending process by NIR spectroscopy and machine vision", European Journal of Pharmaceutics and Biopharmaceutics, 201, 114368, 2024. https://doi.org/10.1016/j.ejpb.2024.114368

[33] Ficzere, M., Péterfi, O., Farkas, A., Nagy, Z. K., Galata, D. L. "Image-based simultaneous particle size distribution and concentration measurement of powder blend components with deep learning and machine vision", European Journal of Pharmaceutical Sciences, 191, 106611, 2023. https://doi.org/10.1016/j.ejps.2023.106611

[34] Fazekas, B., Pogány, D. G., Galata, D. L., Nagy, Z. K., Mészáros, L. A., Hirsch, E. "Characterization of digital camera-based UV illumination fluorescent imaging for concentration measurement with limit of detection, specificity and precision", European Journal of Pharmaceutical Sciences, 210(1), 107117, 2025. https://doi.org/10.1016/j.ejps.2025.107117

[35] Péterfi, O., Mészáros, L. A., Szabó-Szőcs, B., Ficzere, M., Sipos, E., Farkas, A., Galata, D. L., Nagy, Z. K. "UV–VIS imaging-based investigation of API concentration fluctuation caused by the sticking behaviour of pharmaceutical powder blends", International Journal of Pharmaceutics, 655, 124010, 2024. https://doi.org/10.1016/j.ijpharm.2024.124010